Modelling and optimization of residual stress induction on laser-worked X12Cr turbine blades

Festus Fameso * iD

Tshwane University of Technology, Department of Mechanical and Mechatronics Engineering, Pretoria, South Africa, festus.fameso@gmail.com

Dawood Desai iD

Tshwane University of Technology, Department of Mechanical and Mechatronics Engineering, Pretoria, South Africa, desaida@tut.ac.za

Schalk Kok iD

University of Pretoria, Department of Mechanical and Aeronautics Engineering, Pretoria, South Africa, schalk.kok@up.ac.za

Dylan Armfield iD

University of Pretoria, Department of Mechanical and Aeronautics Engineering, Pretoria, South Africa, dylanarmfield@ie-form.ie

Mark Newby iD

Eskom Holdings, Johannesburg, South Africa, newbym@eskom.co.za

Abstract: The energy and power industry conventionally depends on large-scale turbomachinery to meet the ever-growing global energy demands. However, unplanned in-service failures remain a threat to sustainability with safety and economic consequences. The laser shock surface treatment technique is being considered a competitive alternative in mitigating crack initiation and growth, wear and fatigue of industrial components such as turbine blades. This paper presents the modelling and optimization of laser shock treatment parameters using numerical methods and commercial codes such as ABAQUS® and MATLAB®. Model-based process optimization parameters for the induction of global optimum compressive residual stress distribution in laser-worked Chromium-12 based high strength steel alloy (X12Cr) turbine blade is established, showing parametric combinations of inputs variables within the domain under investigation, yielding maximized CRS outputs. A hierarchy of significance of the input parameters to the laser shock peening process for stress induction has also been put forward as an outcome of this study. The capacity to predict and analyze outcomes before actual treatment of the components is beneficial and imperative to cutting costs, downtimes and other economic losses associated with unplanned failure of these components.

Keywords: *Failure, Laser shock peening, Modelling, Residual stresses, Optimization*

Nomenclature	
σ_{HEL}	Hugoniot elastic limit
σ_y	Yield stress
v	Poisson's ratio
ρ	Density
E	Youngs modulus
C	Speed of sound in the material
Γ_0	Gruneisen constant
$\mu;\ \mu_0$	Nominal shear modulus; Shear modulus at 0 Kelvin
g_0	Activation energy
b	Boltzmann's constant
RS	Residual Stress
a, b, d, x, y	Laser peening input parameters
$x_l\ and\ x_u$	Lower and upper bounds of each laser peening input parameter
Z	The global optimization function

1. INTRODUCTION

Turbine blades operate in extremely highly stressed environments, under the action of high thermal and hydrodynamic forces and hence are susceptible to stress and corrosion-induced cracking and fatigue-related failures, most of which are often catastrophic and at times fatal. Laser shock peening (LSP), schematic as shown in Fig. 1, being a developing surface engineering process is now offering an alternative technique to traditional peening methods such as shot peening, to stall or slow down the initializing and evolution of these failure mechanisms by utilizing the dynamics of shock wave energy transfer and propagation in metallic materials to impart compressive residual stresses (CRS) which counteracts against the largely tensile stress and forces acting on the turbine blades while in operation. These CRS increase the material's resistance to a large range of surface-related failures. In comparison with similar surface processing methods, for example, shot peening which uses a succession of high-velocity steel balls to peen the surface of a component, LSP has been shown to achieve deeper levels of residual stresses and lower cold work amplitudes – mainly due to absence of direct contact [1], making it a more beneficial and highly prospective alternative for application in industry.
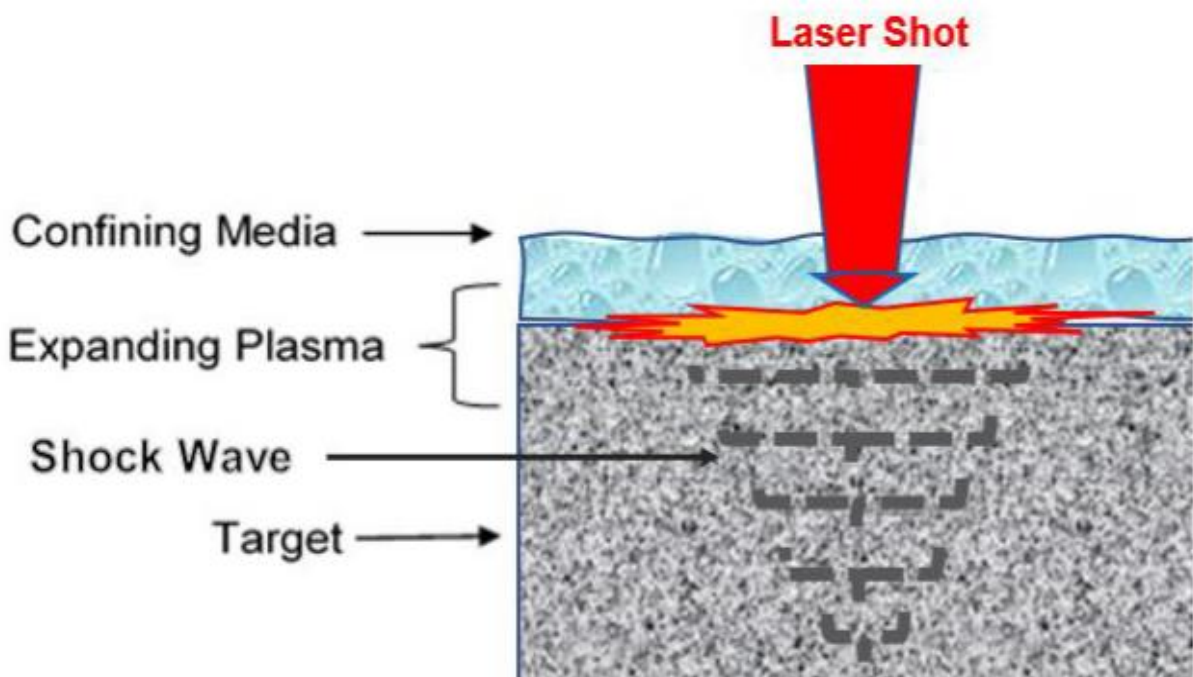

Figure 1. An illustration of the water-confined process of inducing residual stresses in metallic materials by LSP after Ref. [2].

Despite being first proposed and attempted over four decades ago, LSP has only begun to gather and gain more academic curiosity and research attention of late, with the development and ease of use of advanced computing to model, simulate and predict LSP processes using finite element analyses (FEA). According to [2], as opposed to experimental set-ups which are relatively costly and mostly invariable, flexible, time-saving computational models have made the prediction of mechanical effects and responses of metallic materials to laser shot impacts more robust and in-depth, with a wider spectrum of laser peening phenomena now opened for investigation.

Some of the fore-runners of LSP modelling such as Ref. [3] employed the elastic-perfectly plastic (EPP) model to describe the induction of plasticity in a material in the numerical development and analysis of laser peening effects on 35CD4 steel, Ref. [4] have also carried out studies on generating residual stresses by the eigenstrain modelling of arrays of LSP shots, while Ref. [5] investigated overlapping

laser pulse effects during laser shock peening. Ref. [6] successfully performed LSP simulations using the Zerilli-Armstrong (ZA) model, with Ref. [7] going further to conduct optimization studies with the help of laser shock peening simulation-based models, for improved bending fatigue life of Ti–6Al–2Sn–4Zr–2Mo alloy. Refs. [8,10] alongside many others have also implemented LSP simulations using the Johnson-Cook formulation. For instance, Ref. [11] employed the novel physics-based mechanical threshold stress (MTS) model to simulate and determine saturation thresholds for a laser-peen material.

This study thus employs numerical modelling and simulation, using the finite element-based commercial software ABAQUS®, and subsequently gradient-based optimization methods to establish the best combination of laser shot intensity, angle, size, exposure duration and degree of coverage that maximizes the distribution of compressive residual stresses induced in a 12% chromium steel alloy-made last stage steam turbine blade. It goes further to define the ranking of influence and effects of these parameters on residual stresses induction and growth, in the application of LSP as a practicable and effective manufacturing, re-manufacturing, and maintenance process in the industry, especially in the structured and monitored maintenance and prevention of catastrophic failures of turbine blades in the power, energy and aerospace industries.

2. MATERIALS AND METHODS

2.1. Experimental Set-up and Geometric Model

Figure 2. Sections of the cut-out laser peening sample blocks

Cut-out sections as shown in Fig. 2, of X12Cr (Chromium-12 based high strength steel alloy) blocks with chemical composition presented in Table 1, were obtained from out-of-service turbine blades.

Table 1. Chemical composition % grade of X12CrNiMoN12

Element	C	Si	Mn	Ni	P	S	Cr	Mo	V
Composition (% by wt)	0.08 – 0.15	max 0.35	0.50 – 0.90	2.00 – 3.00	max 0.025	max 0.020	11.0 – 12.5	1.50 – 2.00	0.25 – 0.40

The samples, machined into dimensions 20 by 20 by 10 (all in mm) were polished and stress relieved by heat treatment, ensuring the removal of pre-manufacturing and prior internal operating conditions-induced stresses. The samples were then subject to water-confined laser shock peening, but without ablative coating as described by [12], and as will subsequently be modelled computationally. The peening parameters employed are provided in Table 2.

Table 2. Parameters of the laser shock peening procedure.

Laser System	Laser Power Intensity (W/mm^2)	Wavelength (nm)	Laser Beam Energy (J)	Coverage (spots/mm^2)	Spot Size (mm)	% Shot Overlap
Nd:Yag	6×10^{11}	1064	Max. 0.356	20	0.6	83.3

Using the complete abaqus environment (CAE) of the commercial computer-aided analysis software ABAQUS®, a computational replica of the experimental LSP regime was modelled, first with the three-dimensional geometric re-creation of the experimental block samples as shown in Fig. 3.
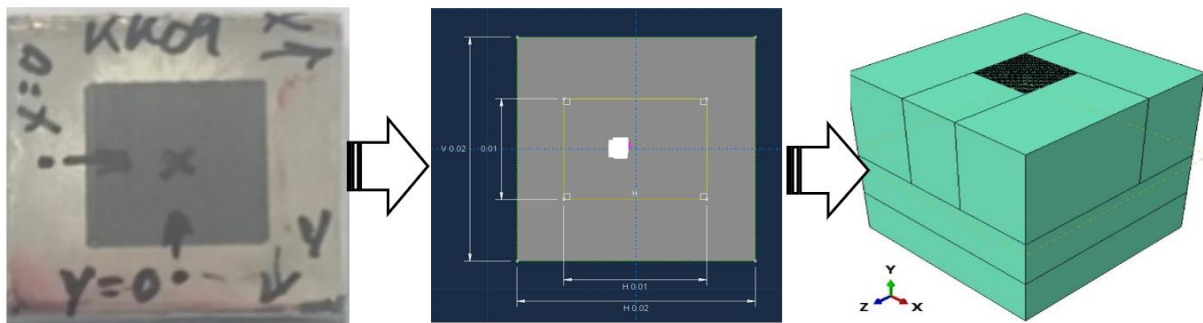

Figure 3. Sections of the cut-out laser peening sample blocks.

A solid homogenously deformable component with concentric cell partitions of dimension 10 mm by 10 mm by 10 mm to accommodate laser shots was created and discretized in the CAE using structured meshing techniques. The discretization allowed for the finite element computation of the stress states in the material, both in the temporal and spatial domains.

2.2. Numerical Modelling

According to Ref. [13], crucial to conducting a parametric study and optimization of the laser shock peening process, it is primarily essential to first perform a single-shot simulation. Consequently, upon validation of its results, an investigation of the effect of multiple shots at close impacts can thereafter be carried out. Modelling LSP numerically takes into account the physical process of high-energy laser shots. These are modelled as high, gigapascal range, short-duration, point pressure loads, impacting a peened surface when irradiated or impacted, and drawing a largely mechanical response from the material. The response manifests in the form of high-amplitude shock waves which grow and is subsequently transmitted into the material. The shock transmission is usually according to the physical laws that govern the constitutive response of the material to such generation and expansion of pressure plasma, and the propagation of the resulting high-intensity shockwave into the metal.

At ultra-high rates of strain in the region of 10^6 per second, which characterizes LSP, the target material behaviour is typified by strain rate jumps, following the stage-wise graduation in plasticity during the process. Unrecoverable deformation prevails up to depths beyond which the peak pressures transmitting through the material ceases to exceed its hugoniot elastic limit. At this point, the stresses become

residuary, as all plastic waves have become fully dissipated, and the energy of the system is at equilibrium. The simulation of this process was conducted using the explicit dynamics code of the commercial FEA program ABAQUS® using the method described by [14] for first the single shot analysis and subsequently for multiple shots analysis. The sequence of the process of carrying out the numerical analysis is illustrated in Fig. 4.
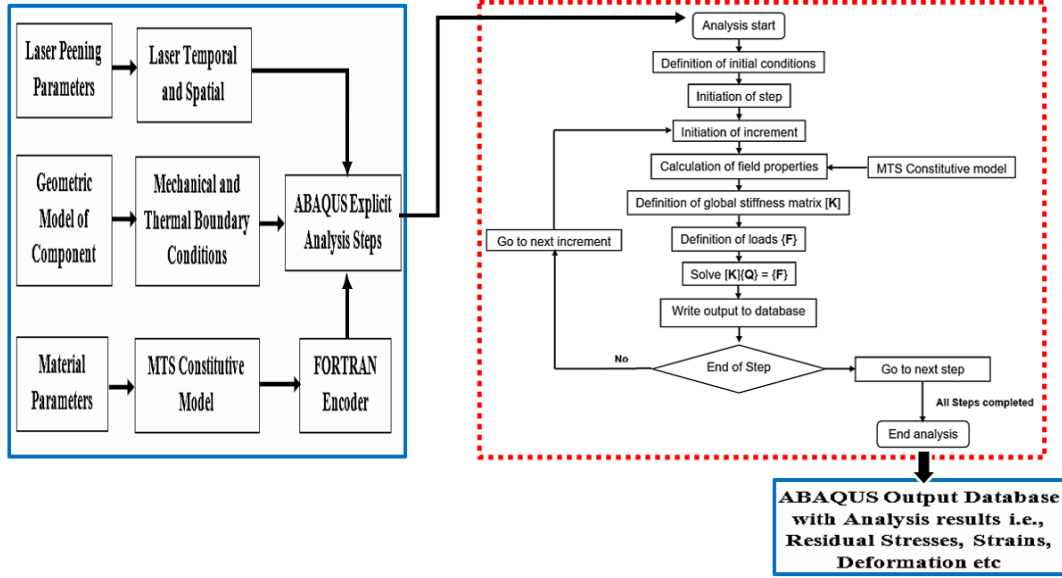

Figure 4. The sequence of analysis and numerical prediction of residual stresses induced by LSP.

The constitutive formulation of the LSP process, which includes shock pressure evolution and propagation, hydrodynamic pressure compaction, and material plasticity at high rates of strain where captured by the coupling of the elastoplasticity limit formulation, hydrodynamic equation of state as defined by Mie-Gruneisen and a stress threshold constitutive model given in Eqs. (1–3) respectively by,

$$\sigma_{HEL} = \sigma_y \frac{(1-v)}{1-2v}, \tag{1}$$

$$P = \frac{\rho_0 C_0^2 (\eta-1)[\eta - \frac{\Gamma_0}{2}(\eta-1)]}{[\eta - \tilde{S}(\eta-1)]^2} + \Gamma_0 \bar{e}, \tag{2}$$

$$\sigma_y(\epsilon_p, \dot{\epsilon}_p, T) = \sigma_a + (S_i \sigma_i + S_e \sigma_e) \frac{\mu(P,T)}{\mu_0}, \tag{3}$$

where S establishes the thermophysical effects of the mechanical threshold stress model as a representation of the strain-rate dependent scaling factor obtained in (4) as follows:

$$S = 1 - (\frac{kT}{g_0 \mu b^3 b \ In \ \dot{\epsilon}_0/\dot{\epsilon}})^{1/q})^{1/p}) \tag{4}$$

Where σ_{HEL} is the Hugoniot elastic limit, σ_y is the material yield stress = 870 MPa, v is the poisons ratio = 0.3, ρ is the material density = 7700 kg/m3, E is the Youngs modulus = 204 GPa. C is the speed of sound in the material = 4313 m/s, Γ_0 is the Gruneisen constant = 1.4545 and μ =85 GPa is the nominal shear modulus and μ_0 =71 GPa is the shear modulus at 0 Kelvin. The internal energy per unit volume of the material and hydrostatic pressure are, $\bar{e}$ and P respectively, while g_0 and b likewise denote the activation energy and Boltzmann's constant respectively.

2.3. Numerical Optimization

Using the finite element model, simulations were carried out with combinations of parameters of the five LSP inputs under consideration. The range of these parameters which formed the five to six levels of design variables of the optimization process are 0 to 75 degrees of shot angle, 0 to 100% of overlap of shots, 0.2 to 1 mm of laser shot diameter, 2 to 10 GW/cm^2 of the intensity of laser shots and 5 to 25 nanoseconds of full-width half-maximum peak exposure duration. The results of these simulations generated a stack of residual stress and surface roughness results which by multiple regression methods are used to generate a residual stress fitness function which approximates the finite element model having satisfied the error requirements. The residual stress optimization fitness function is presented in (5);

$$\begin{aligned}
RS = ((((5.3577e8) &- ((4.16455e6)a) - ((7.63825e6)\,b) + ((1.77108e7)\,d) \\
&- ((9.90105e7)\,x) - ((2.25138e7)\,y) - (5705.33042\,a\,b) \\
&+ ((9.61880e6)(a\,d))((4.90863e5)(a\,x)) + ((1.43549e5)a\,y) \\
&- ((3.46876e5)\,b\,d)((1.27044e5)\,b\,x)((5.00322e5)b\,y) \\
&- ((3.06403e7)\,d\,x) - ((2.23868e7)\,d\,y) + ((2.90996e6)\,x\,y))
\end{aligned} \tag{5}$$

where a is the angle of laser shot impact in degrees, b is the degree of overlaps in percentage, d is the diameter of the laser beam at the point of impact in mm. x and y represents the intensity of the laser shot in GW/cm^2 and FWHM peak exposure time in nanoseconds respectively.

As shown in Fig. 5, the fitness function was set up for optimization as the objective function of a gradient-based optimization, using the function minimizer including constraints (FMINCON) module of the MATLAB® optimization toolbox, a solver-based non-linear optimization algorithm which finds the minimum or maximum of a constrained nonlinear multivariable function. The objective was set at obtaining the set and combination of parameters from the range of design variables under consideration that maximizes the residual stress (RS) outcomes within the constraints of minimum surface roughness (Ra) values. Thus, the optimization task was numerically set up as (6);

$$Min\,Z = Min(-f(RS)) \tag{6}$$

Here, subject to $C_i(x) \leq RS$; $bx_l \leq \in x \to X \leq bx_u$; global domain bounds exists.
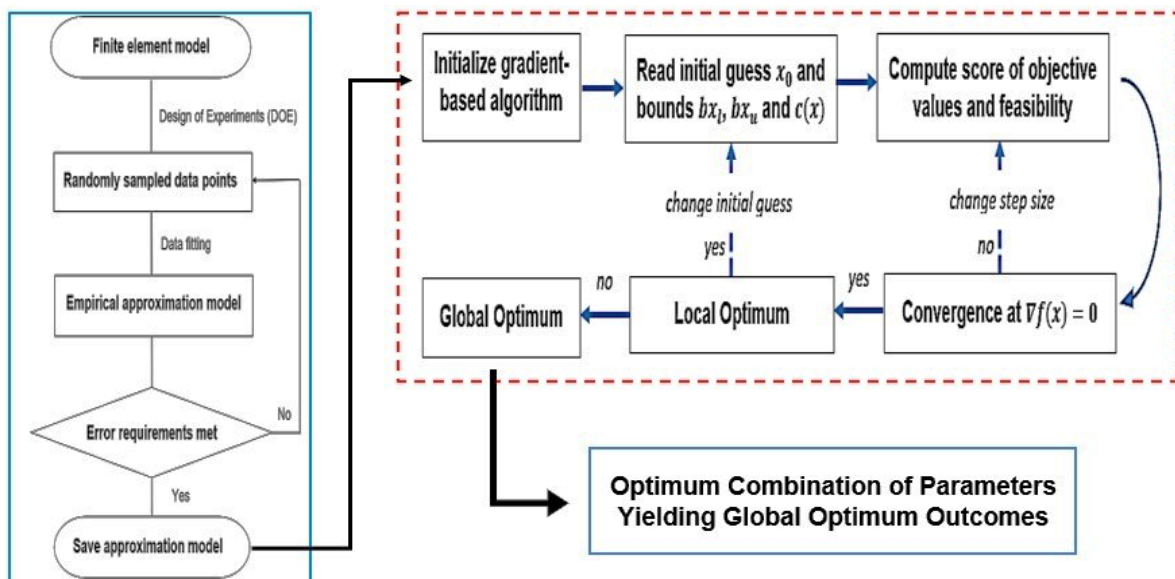

Figure 5. The flow of gradient-based optimization from a FE LSP residual stress prediction model.

3. RESULTS AND DISCUSSION

The results of the validation of the LSP simulation model against the experimental study described in the previous section are presented in Fig. 6. The stress-to-depth profiles of the peening end state of the treated specimen, measured radially and axially after dynamic energy equilibrium had been attained in the computational domain. These were benchmarked with stress-to-depth profiles obtained utilizing combined electropolishing and x-ray analysis, on completion of the shock peening sequence, in the experimental set-up. They showed promisingly close correlation and less than 10% deviations in the computed values of in-depth residual stress and indentation by the laser shock treatment of the X12Cr steel.
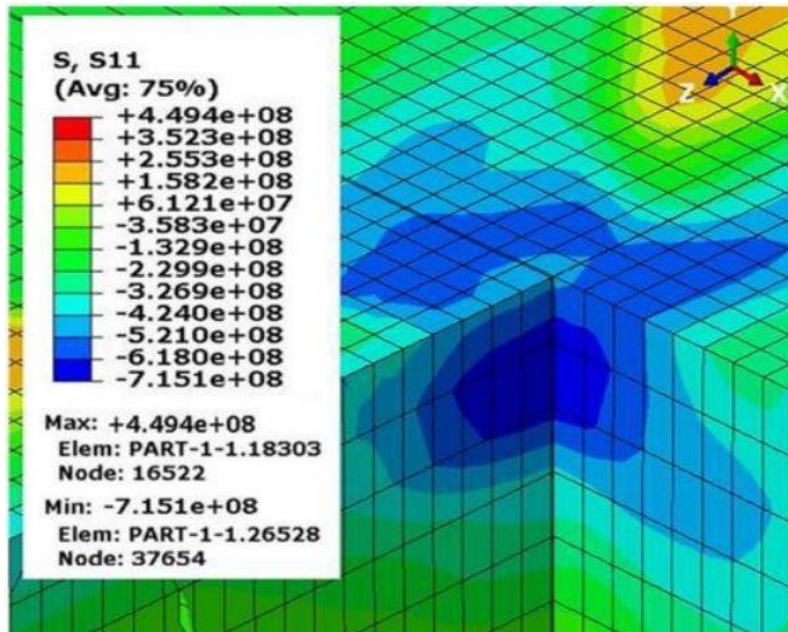
(a)
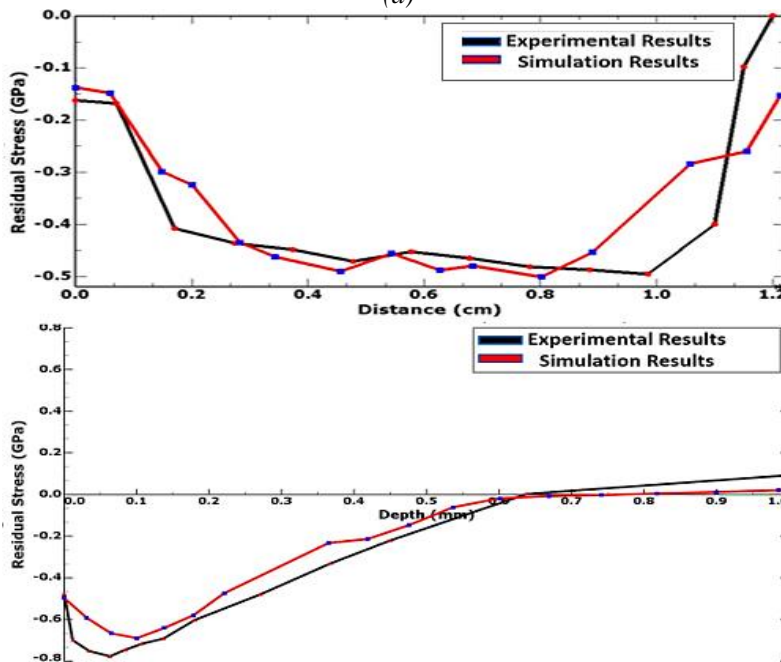
(b)

Figure 6. Validation of LSP simulation results against experiment: (a) In-plane S11 (σ_{xx}) stresses induced by 6GW/cm2, 20 spots/mm2 density and 15 ns FWHM peak. (b) Simulation vs Experiment benchmark for both surface and in-depth residual stress results.

As illustrated in Fig. 5, having provided a validation of the FE model, its mathematical surrogate, presented in Eq. (5), was obtained by data fitting and regression analyses and tested for its degree of accuracy in approximating the FE model. Using error analyses methods to compare residuals and deviations, the surrogate model replicated the results of the FE model to an appreciably close degree of correlation as presented in the plot of residuals illustrated in Fig. 7. The generality of the data points of the actual and the simulated (predicted) results fall on or close enough to the red line.
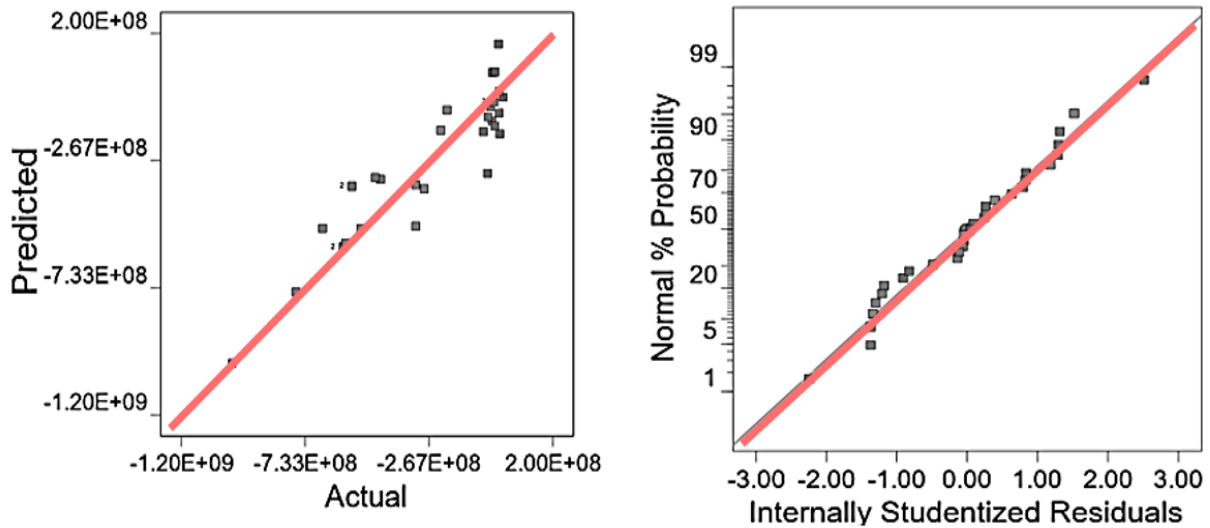

Figure 7. Analysis of residuals in the verification of the approximation capacity of the surrogate model to the FE model.

The internally studentized residuals present the number of standard deviations that separate the actual and predicted response values. The red line in this instance is a diagonal line that would normally represent a perfect fit where the predicted result equals the actual result from the experimental benchmark, hence the closer to the diagonal, the more accurate the prediction by the approximation model. Consequent upon the validation of the models, the fitness function was subjected to optimization to obtain the sets of combination of parameters that produces the optimum (maximized) value of CRS. The optimization search, using a gradient-based approach and random selection of initial values in the confines of the lower and upper domains of the design variables yielded local optimums between 1.14 GPa, and 1.42 GPa, with the latter selected and designated as the global optimum after a further 50 iterations yielded no response value of higher magnitude. Normality testing which was carried out on the influence of each of the 5 design variables under investigation, resulted in their absolute effect estimates in descending order of influence on yielding maximized CRS. Fig. 8, showing the half-normal plot of effects, presents the result of this analysis.
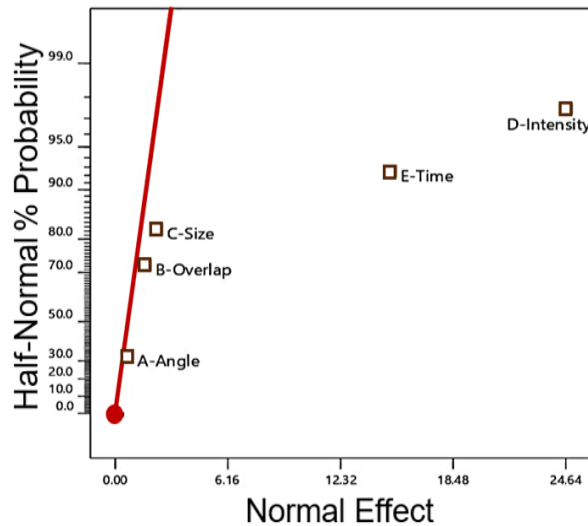
Figure 8. Normality plot illustrating the ranking of effects and influence of each LSP input factor on residual stress induction.

The red diagonal in this instance, which is the half-normal % probability reference line, fits the smallest 50% of the effects. This means that the farther an effect from the line, the more significant it is to the desired outcome of the process. The absolute values in normal effect increase from the left to the right of the abscissa, indicating increasing order of significance of the input parameters, acting independently, or combined, on the desired outcome of obtaining optimum CRS magnitudes. The shot intensity is observed to be the most significant factor while the shot angle is the least. The local optima were plotted against the design variables with the most significant influence on compressive residual stress according to the hierarchy of effects analysis. The resulting response plots as shown in Fig. 9, reveal that possible combination of design parameters that optimizes the desired CRS output.
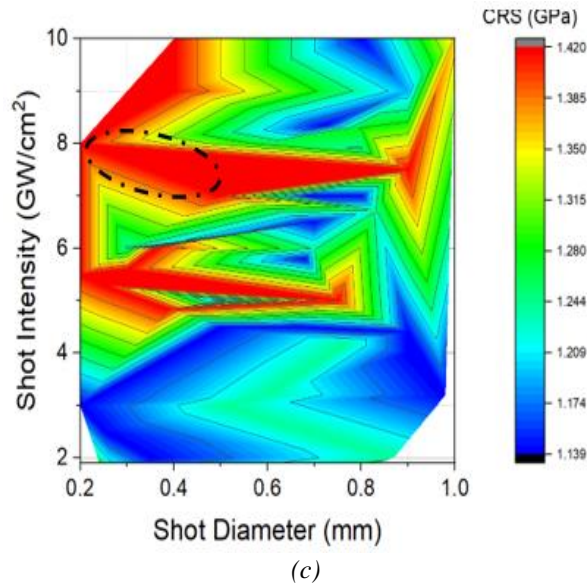

(a)   *(b)*

(c)
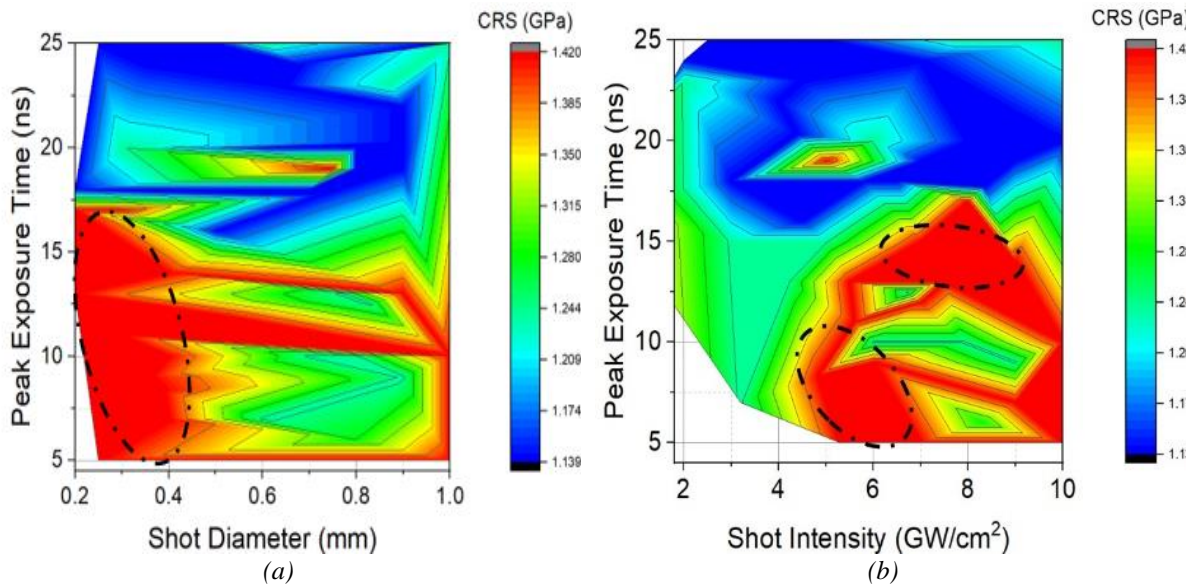
Figure 9. Response plot of feasible optimums and the design combinations that yield the optimum value: (a) Peak exposure time vs Shot Diameter, (b) Peak exposure time vs Shot intensity, (c) Shot intensity vs Shot diameter

The global optimum results as shown by the ringed regions with red contour colors show that combinations of parameters within the range of 6 – 8 GW/cm^2 of shot intensity, 0.3 to 0.5 mm of shot diameter and FWHM peak exposure times of between 5 – 15 ns enhance the generation and induction of optimum magnitudes of CRS as a priority in a laser shock peening operation.

4. CONCLUSION

In conclusion, a numerical analysis of the modelling and parameter optimization of residual stress induction in X12Cr turbine blade material by laser-shock surface treatment has been presented in this study. The most influential of five input factors under consideration, i.e. the shot intensity, size, angle, degrees of overlap and peak exposure duration, to residual stress induction has been investigated and the combination of parameters that will yield the optimum compressive residual stress induction has been explored. By finite element methods, residual stress induced by an LSP process has been predicted via simulations. A surrogate model which is empirically representative of and can be substituted for the FE model was developed and used to set up a gradient-based optimization computation. The optimization ciphering arrived at parametric combinations of inputs within the range of 6 – 8 GW/cm^2 of shot intensity, 0.3 to 0.5 mm of shot diameter and FWHM peak exposure times of between 5 – 15 ns which will yield a global optimum CRS induction in a peening operation.

Furthermore, the input variables have been established to show a descending hierarchy of significance to the generation of the desired outcomes, with shot intensity being the most influential, followed by the duration of exposure, the size, the degree of overlaps and the shot angle being the least influential. Such structured knowledge of LSP application in industry is essential to the success of the evolution and implementation of strategic, methodical, and structured health and condition monitoring of the useful life of critical components such as turbine blades. As promoted by this study, the capacity to predict and analyse LSP outcomes before actual treatment of the components is beneficial and imperative to cutting costs, laser peening treatment time scales, downtimes and other economic losses which result from the unplanned in-service failure of these components.

Acknowledgement

REFERENCES

[1] Peyre, P., Chaieb, I., Braham, C. FEM calculation of residual stresses induced by laser shock processing in stainless steels. *Modelling and Simulation in Materials Science and Engineering* 2007; *15*(3): 205–221. doi 10.1088/0965-0393/15/3/002.

[2] Fameso, F.; Desai, D.; Kok, S.; Armfield, D.; Newby, M. Residual Stress Enhancement by Laser Shock Treatment in Chromium-Alloyed Steam Turbine Blades. *Materials* 2022; *15*; 5682. https://doi.org/10.3390/ma15165682

[3] Braisted, W., Brockman, R. Finite element simulation of laser shock peening. *International Journal of Fatigue* 1999; *21*: pp. 719–724.

[4] Achintha, M., Nowell, D. Eigenstrain modelling of residual stresses generated by arrays of LSP shots. *Procedia Engineering* 2011; *10*: 1327–1332. https://doi.org/10.1016/j.proeng.2011.04.221

[5] Karbalaian, H. R., Yousefi-Koma, A., Karimpour, M., Mohtasebi, S. S. Investigation on the Effect of Overlapping Laser Pulses in Laser Shock Peening with Finite Element Method. *Procedia Materials Science* 2015; *11*: 454–458. https://doi.org/10.1016/j.mspro.2015.11.045

[6] Amarchinta, H. K., Grandhi, R. v., Langer, K., Stargel, D. S. Material model validation for laser shock peening process simulation. *Modelling and Simulation in Materials Science and Engineering* 2009; *17*(1): 0–15. https://doi.org/10.1088/0965-0393/17/1/015010

[7] Bhamare, S., Ramakrishnan, G., Mannava, S. R., Langer, K., Vasudevan, V. K., Qian, D. Surface & Coatings Technology Simulation-based optimization of laser shock peening process for improved bending fatigue life of Ti – 6Al – 2Sn – 4Zr – 2Mo alloy. *Surface & Coatings Technology 2013*; *232*: 464–474. https://doi.org/10.1016/j.surfcoat.2013.06.003

[8] Jiang, Y. F., Ji, B., Gan, X. D., Hua, C., Li, X., & Zhu, H. Study on the effect of laser peening with different power densities on fatigue life of fastener hole. *Journal of Optics and Laser Technology* 2018; *106*: 311–320. https://doi.org/10.1016/j.optlastec.2018.04.025

[9] Keller, S., Chupakhin, S., Staron, P., Maawad, E., Kashaev, N., Klusemann, B. Experimental and numerical investigation of residual stresses in laser shock peened AA2198. *Journal of Materials Processing Technology* 2018; *255*: 294–307. https://doi.org/10.1016/j.jmatprotec.2017.11.023

[10] Zhao, J., Dong, Y., Ye, C. Laser shock peening induced residual stresses and the effect on crack propagation behaviour. *International Journal of Fatigue* 2017; *100*: 407–417. https://doi.org/10.1016/j.ijfatigue.2017.04.002

[11] Fameso, F., Desai, D., Kok, S., Newby, M., Glaser, D. Simulation of laser shock peening on X12Cr steel using an alternate computational mechanical threshold stress plasticity model. *The International Journal of Advanced Manufacturing Technology* 2020; *111*(1): 1– 11. https://doi.org/10.1007/s00170-020-06079-y.

[12] Kuveya, KR., Polese, C., Newby, M. Laser Peening versus Shot Peening Effects on Residual Stress and Surface Modification of X12CrNiMo12 Turbine Blade. In: 6th International Conference on Laser Peening and Related Phenomena; 6 – 11 November 2021: South Africa.

[13] Karbalaian, H. R., Yousefi-Koma, A., Karimpour, M., Mohtasebi, S. S. Investigation on the Effect of Overlapping Laser Pulses in Laser Shock Peening with Finite Element Method. *Procedia Materials Science* 2015; *11*: 454–458. https://doi.org/10.1016/j.mspro.2015.11.045

[14] Fameso, F., Desai, D. Explicit analysis using time-dependent damping simulation of one-sided laser shock peening on martensitic steel turbine blades. *Simulation* 2020; *96*(12): 927–938. https://doi.org/10.1177/0037549720954272